Journal of Geochemical Exploration 168 (2016) 150–162

Contents lists available at ScienceDirect

Journal of Geochemical Exploration

journal homepage: www.elsevier.com/locate/gexplo

Stepwise regression for recognition of geochemical anomalies: Case study in Takab area, NW Iran

Ahad Nazarpour [a,*], Ghodratolah Rostami Paydar [a], Emmanuel John M. Carranza [b,c]

[a] Department of Geology, College of Sciences, Ahvaz Branch, Islamic Azad University, Ahvaz, Iran
[b] Economic Geology Research Centre, James Cook University, Townsville, Queensland, Australia
[c] Institute of Geosciences, State University of Campinas, Campinas, São Paulo, Brazil

ARTICLE INFO

Article history:
Received 28 October 2015
Revised 19 June 2016
Accepted 3 July 2016
Available online 05 July 2016

Keywords:
Stepwise regression
Geochemical exploration
Geochemical anomaly
Logratio transformation
Takab

ABSTRACT

Stream sediment geochemical data represent compositional materials derived from various sources, including single or multiple lithologic units, soil types, rocks types, etc. In order to delineate geochemical anomalies, stream sediment geochemical data are usually subjected to suitable multivariate analysis, and not simply using univariate threshold values because these are not reliable for delineation of geochemical anomalies in areas with complex geological units. Relationships among multiple major/trace elements and rock types are more important than single major/trace elements for delineation of geochemical anomalies. In this study we present an approach based on robust stepwise multiple regression using values major oxides (SiO_2, Al_2O_3, Fe_2O_3, MnO, and MgO) in stream sediments to predict elemental content related to rock types and to recognize geochemical anomalies. The major/trace element data were subjected to isometric logratio transformation to address the compositional data closure problem. For further examination of the stepwise regression method, its performance was compared to robust principal components analysis (RPCA), median + 2MAD and concentration-area (C-A) fractal methods. The results show that multi-element anomalies obtained by the stepwise regression method, compared to those obtained by the other methods, have stronger spatial association with the known deposits, such as Chichaklo and Ay-Ghale-Si in the Takab 1:25,000 scale geological map (NW) Iran, and the anomalies have stronger spatial correlation with structural features and prospects, and thus can be used as guides to new exploration targets.

1. Introduction

Recognition of anomalous and background values in a stream sediment geochemical dataset is one of the basic tasks in mineral exploration. An anomaly can be defined as a concentration of element or metal that is greater than a threshold concentration value (i.e., upper limit of background population). Stream sediments are composite materials derived from the weathering and erosion of one or more sources upstream of a sample site. Therefore, uni-element contents of stream sediments are derived from multiple (usually background and rarely anomalous) sources. In most cases, a major proportion of variation in uni-element contents in stream sediment is due to lithological units underlying the areas upstream of stream sediment sample sites (Carranza, 2010b). Recognition of anomalies from background in a regional-scale stream sediment geochemical dataset is an important stage of mineral exploration to delineate potential areas for detailed investigation at finer scales (Deng et al., 2010; Nazarpour et al., 2015c; Pazand et al., 2011; Rantitsch, 2000; Shamseddin Meigoony et al., 2014; Rezaei et al., 2015).

Various statistical methods have been used to process geochemical data in order to determine threshold values. Statistical quantities, such as the mean, standard deviation (sdev) and percentiles, have been used to define threshold for separating anomalies form background. For example, geochemical anomalies have been defined as values greater than a threshold defined as the 75th or 85th percentile, and mean + 1sdev or mean + 2sdev. Based on such statistical quantities, there are two main groups of methods for determining threshold values: the first group includes frequency-based univariate methods such as mean ± 2sdev (Hawkes and Webb, 1962), probability graphs, box-plot and Q-Q plot (Govett et al., 1975; Miesch, 1981; Sinclair, 1976; Stanley and Sinclair, 1989) and second group includes variance-based multivariate methods to define anomalous multi-element associations (e.g., Aitchison, 1986; Nazarpour et al., 2015a and b).

The application of a single uni-element threshold value, defined by frequency-based methods, to delineate anomalies often results in false-negative anomalies in areas with low background values or false-positive anomalies in areas with high background values, thereby undermining the utility of geochemical exploration to define new targets. A reasonable way to solve this problem is to determine the

* Corresponding author.
E-mail addresses: Ahad.nazarpour@gmail.com, A.nazarpour@ahvaziau.ac.ir (A. Nazarpour).

http://dx.doi.org/10.1016/j.gexplo.2016.07.003
0375-6742/

underlying relationships among geochemical anomalies and plausible causative geological processes. Using rock types to represent geological processes is a common logical solution tool to recognize geochemical anomalies in complex geological settings or in overburden-covered areas (Hao et al., 2014), because there is often a clear relationship between rock types and major oxide content of rocks (Cohen et al., 2012; Reimann and Garrett, 2005). For elimination of lithological effects on uni-element data, one can use a multiple regression model to estimate element values and then subtract these values from measured element values to yield *geochemical residuals* that may or may not be related to anomalous sources (Bonham-Carter and Goodfellow, 1986; Hao et al., 2014).

Another main limitation of the above-mentioned methods is that they do not take into account the variability of spatial-statistical distribution of geochemical data. However, different areas can differ in rock compositions or have experienced different geological processes, which result in different geochemical thresholds. Therefore, the above-mentioned methods are of limited use in situations where there are extensive overlaps between background and anomalous values, or where weak anomalous values are hidden within the strong variance of background (Cheng, 2007).

The spatial-statistical distribution of geochemical data can be characterized using fractal geometry (Mandelbrot, 1983), which is a branch of non-linear mathematics that has been widely applied in the geosciences (e.g., Afzal et al., 2010; Agterberg et al., 1993; Ali et al., 2007; Carranza, 2008; Cheng et al., 1994; Deng et al., 2010; Sim et al., 1999; Turcotte, 1986; Wei and Yang, 2010). Several fractal and multifractal models, including concentration-area (C-A) (Cheng et al., 1994, Nazarpour et al., 2015a), spectrum-area (S-A) (Cheng, 2004; Cheng et al., 2000; Xu and Cheng, 2001), concentration-distance (C-D) (Li et al., 2003), concentration-volume (C-V) (Afzal et al., 2011) and number-size (N-S) (Agterberg, 1995; Deng et al., 2010; Mandelbrot, 1983; Turcotte, 2002; Wang et al., 2010), have been developed for various applications in the geosciences including analysis of geochemical data.

In addition to the above-mentioned main limitations of frequency- and variance-based methods for anomaly recognition, geochemical data are compositional (i.e., contribution of parts to some whole), which carry exclusively relative information (Aitchison, 1986). For example, if the SiO_2 content of an igneous rock is 68% of the whole weight, then the value of MgO will only be equal to or <32%. This means that geochemical data are not absolute values, but only provide relative information of certain element in a whole sample (Aitchison, 1986). Therefore, compositional data represent a closed number system and should be opened prior to understanding of realistic relationships among compositions (Filzmoser et al., 2009; Carranza, 2011; Nazarpour et al., 2015b). Therefore, it is crucial to apply an appropriate transformation to geochemical data prior to using any method of multivariate analysis. The log-ratio (logarithm of a ratio) transformation methodology proposed by Aitchison (1986) represents a powerful set of techniques to open compositional data. Three log-ratio transformations have been proposed for opening of compositional data: (1) additive log-ratio (alr) transformation (Aitchison, 1986); (2) centered log-ratio (clr) transformation (Aitchison, 1986) and (3) isometric log-ratio (ilr) transformation (Egozcue et al., 2003). These transformations allow for the application of standard statistical methods to transformed data, although with some limitations or modifications. In this study, the stream sediment geochemical data were ilr-transformed prior to statistical analysis.

Finally, exploration geochemical data typically comprise a large set of geochemical variables (e.g., major oxides, trace elements/metals) and the choice of which of these variables can be used as predictor (or independent) and response (or target) variables is a common problem in attempting to describe relationships among such variables through regression analysis. However, considering that lithology is a major source of variation of trace elements/metals and that lithological units are composed of various major oxides (e.g., SiO_2, Al_2O_3, Fe_2O_3, MnO, and MgO), major oxides are typically used as predictor variables in lieu of lithological units. Determining the most significant predictor variables, and therefore reliable estimates of element values, can be achieved through stepwise multiple regression.

This paper focuses on the identification of geochemical anomalies in the Takab 1:25,000 scale geological map sheet by using stream sediment geochemical data to derive geochemical residuals of trace elements, which would indicate areas of enrichment (e.g., due to mineralization) or depletion. Previous researches have derived geochemical residuals by applying stepwise multiple regression using trace elements as dependent variables (or targets for exploration) and areal proportions of lithologic units as independent variables (predictors) or as proxies of the influence of lithology on trace element background concentration (Bonham-Carter and Goodfellow, 1984, 1986; Carranza and Hale, 1997; Moon, 1999; Carranza, 2010a,b). However, we argue that using areal proportion of lithologic units as predictors would depend on the availability of a geological map and the results would vary depending on the scale of the lithologic map used. In this paper, we used major elements as independent variables (predictors) or as proxies of the influence of lithology on trace element background concentration. Results from this proposed methodology are validated using lithogeochemical data and by comparing with results from using the median + 2MAD for exploratory data analysis (EDA), concentration- area (C-A) fractal model and robust principal component analysis (RPCA) as two effective approaches to separate geochemical anomalies from background in stream sediment geochemical compositional data.

2. Methods

2.1. Exploratory data analysis (EDA)

In EDA of geochemical exploration data, the median + 2MAD value was originally used to identify extreme values and act as threshold for further inspection of large data sets (Hawkes and Webb, 1962; Zheng et al., 2014). The EDA was first established by Tukey (1977), was developed further by Kürzl (1988), and then was used by many researchers in modeling of geochemical anomalies (e.g., Ali et al., 2007; Carranza, 2008, 2010a,b; Nazarpour et al., 2014). The *MAD* is the median of absolute deviations of individual dataset values (X_i) from the median of all dataset values (Tukey, 1976):

$$MAD = median|X_i - median(X_i)|. \quad (1)$$

2.2. Concentration-area (C-A) fractal model

The C-A fractal model was first introduced by Cheng et al. (1994) for recognition of geochemical anomalies from background. It has the following general forms (Cheng et al., 1994):

$$A(\rho \le \upsilon) \propto \rho^{-a_1}; A(\rho > \upsilon) \propto \rho^{-a_2} \quad (2)$$

where $A(\rho)$ denotes area with background concentrations (ρ) less than or equal to a threshold concentration (υ) or area with anomalous concentrations (ρ) greater than the threshold concentration (υ), a_1 and a_2 are slopes of straight lines fitted to log-log plots of ρ versus $A(\rho)$.

Cheng et al. (1994) proposed two approaches to calculate $A(\rho)$: (1) the $A(\rho)$ is area enclosed by a contour of concentration value (ρ) on a geochemical map derived by interpolation of the original concentration values using a weighted moving average method; and (2) $A(\rho)$ is obtained by application of the box-counting method to the original concentration values. Distinct patterns, each corresponding to a set of

similarly-shaped contours, can be separated by different straight segments fitted to the values of the contours and enclosed areas on log-log plot of $A(\rho)$ versus ρ. The slopes of individual fitted straight lines can be estimated by the exponents of the power-law relations in Eq. (2). The optimum threshold for separating anomalies from background is the concentration value common to two fitted straight lines on the log-log plot.

2.3. Robust principal components analysis (RPCA)

Geochemical data are multivariate in nature, meaning that background and/or anomalous populations depict associations of at least two elements/metals. Certain techniques can be used to reveal inter-element associations in a multivariate dataset. Classical factor analysis (PCA) is one of the most popular methods of multivariate data analysis (Jolliffe, 2002; Reimann et al., 2002; Wang and Zuo, 2015). In many practical applications, log-transformation is applied in order to reduce data skewness so that the variables approximately follow a normal distribution. However, log-transformation does not accommodate the compositional nature of the data. In addition, geochemical data usually contain outliers (i.e., values that do not follow the main data structure) and are heterogeneous, and these severely affect classical estimators (e.g., arithmetic mean, sample covariance matrix) and can render results of classical PCA meaningless (Filzmoser et al., 2010; Locantore et al., 1999; Wang and Zuo, 2015). The compositional nature of geochemical data and the presence of outliers could severe influence the results of standard statistical methods such as PCA. The main reason is that both the arithmetic mean and simple covariance matrix, which are used in most multivariate statistical procedures, are very sensitive to deviations from the main data structures. In order to reduce the effect of the above-mentioned features, especially of outliers, robustness in PCA can be achieved by replacing the arithmetic mean and the simple covariance matrix by their robust counterparts. A frequently used robust estimator of location and covariance is the minimum covariance determinant (MCD) estimator, and so the robust PCA (RPCA) based on minimum covariance determinant (MCD) estimator can overcome the shortcomings of classical PCA.

Because geochemical data are compositional in nature, they represent a closed number system. Therefore, a data transformation is required to properly reveal inter-element relationships prior to analysis (Asadi et al., 2014; Carranza, 2011; Nazarpour et al., 2015b; Wang and Zuo, 2015; Zuo et al., 2013b). The following log-ratio transformation methods, namely alr (Eq. (3)), clr (Eq. (4)), and ilr (Eq. (5)) have been suggested to 'open' compositional data (Egozcue et al., 2003; Filzmoser et al., 2009):

$$y_i = \log\frac{x_i}{x_D} \quad (i = 1,2,\ldots,D-1) \tag{3}$$

$$y_i = \log\frac{x_i}{\sqrt[D]{\prod_{i=1}^{D} x_i}} \quad (i = 1,2,\ldots,D) \tag{4}$$

$$y_i = \sqrt{\frac{D-i}{D-i+1}}\log\frac{x_i}{\sqrt[D-1]{\prod_{j=i+1}^{D} x_j}} \quad (i = 1,2,\ldots,D-1) \tag{5}$$

For alr-transformation, one compositional part is selected to divide the remaining parts, and then the ratios are log-transformed (Aitchison, 1986). For clr-transformation, every value is divided by the geometric mean of all values and the ratios are log-transformed. However, clr-transformation results are collinear because the sum of values of every clr-transformed variable is zero. The ilr-transformation can overcome this shortcoming and give correct representation of compositional data in (D-1)-dimensional Euclidean real space.

In this study, the stream sediment geochemical data were ilr-transformed prior to RPCA (Filzmoser et al., 2009). However, because ilr-transformed variables do not represent a one-to-one transformation from the simplex to the standard Euclidean space, the results of RPCA to extract geochemical anomalies can be back-transformed to clr space for better interpretation. The analysis was completed using the "robCompositions" and "spatial" which are free R packages (see http://cran.r-project.org/). In RPCA, we applied the Kaiser (1960) criterion (i.e., eigenvalue > 1) to retain only the statistically meaningful PCs that can be extracted from the data.

2.4. Stepwise regression model to selection of estimator variables

In regression analysis, the relationship, called the regression function, between a dependent variable (Y) and several one or more independent or predictor variables (X_i) can be defined. A regression model with at least one predictor variable is a multiple regression model. A multiple linear regression model, using trace elements are dependent variables and major oxides as predictor variables, can take the following general form:

$$C_i = \alpha + \beta_i \times C_{SiO_2} + \beta_2 \times C_{Fe_2O_3} + \ldots + \beta_k \times C_k + \varepsilon \text{ for } i = 1,\ldots,n \text{ samples} \tag{6}$$

$$C_i = \alpha + \sum_{j=1}^{k}\beta_j C_j + \varepsilon \tag{7}$$

where C_i is measured value of dependent trace element in sample i, C_j is measured value of predictor major oxide j in sample i, α and β are undetermined coefficients, and ε refers to summation of the influence of all associated random factors (sometimes referred to as random errors). Random error terms are assumed to be independent, and follow the normal distribution with mean 0 and covariance δ^2. Predicted values of C_i, denoted as C_i, can be derived by determining coefficients α and β through a least square method, thus:

$$C_i = \alpha + \beta_1 \times C_{SiO_2} + \beta_2 \times C_{Fe_2O_3} + \ldots + \beta_k \times C_k \tag{8}$$

and geochemical residuals (e_i), which may be positive or negative, for sample i, can be derived as:

$$e_i = C_i - C_i \tag{9}$$

To determine the relative contribution of each predictor variable in their ability to account for total variation of the dependent variable, one can perform a forward, stepwise solution, but force every predictor variable into the solution either simultaneously or sequentially. In this way, one can systematically evaluate the effect of each predictor variable. At the end of each step in a sequential or stepwise linear regression, the predictor variables that significantly contribute to the prediction of C_i can be identified and this procedure continues until non-significant predictor variables are eliminated for each of the favorable elements. Statistical criteria inclusion or exclusion of predictor variables in a final linear regression model are discussed in detail in, for example, Shacham (1999) and Shacham and Brauner (2003).

Stepwise multiple regression has been used to model the relationship between trace element concentrations in stream sediments and rock types in areas where geological maps are available (e.g., Bonham-Carter and Goodfellow, 1984, 1986; Bonham-Carter et al., 1987; Carranza and Hale, 1997; Moon, 1999; Carranza, 2010a,b). However, variations in major element concentrations in stream sediments are invariably due to lithology (De Vivo et al., 1998; Ohta et al., 2005). Therefore, in this study, instead of using areal proportions of lithologic units as proxies of lithologic influence (e.g., Bonham-Carter and Goodfellow, 1984, 1986; Bonham-Carter et al., 1987; Carranza and Hale, 1997; Moon, 1999; Carranza, 2010a,b), we used concentrations of major oxides (SiO_2, Al_2O_3, MnO, Fe_2O_3) as predictor variables of trace metal concentrations using stepwise regression. Finally, derived

geochemical residuals (e_i) (Eq. (9)) are subjected to PCA and then C-A fractal analysis for separation of multi-element geochemical anomalies.

3. Geological setting and mineralization of the study area

The Takab 1:25,000 scale geological map sheet is located in the eastern part of the Takab 1:100,000 scale geological map sheet, which is in the NW part of Iran (Nabavi, 1976). The volcanic arc and the Sanandaj-Sirjan metamorphic zone in NW Iran (Fig. 1) were formed due to the continental collision between the Iranian micro-continent and the Afro-Arabian continent during closure of the Tethys ocean in the Late Cretaceous (Ghasemi and Talbot, 2006; Karimzadeh Somarin, 2005; Mohajjel and Fergusson, 2000). More specifically, these belts were formed as a result of subduction of the Arabian plate beneath central Iran during the Alpine orogeny (Agard et al., 2005). In two separate time intervals, one during Late Precambrian–Early Cambrian and the other during Tertiary (Neogene), the prevailing geological (namely, tectonic, magmatic, metamorphic, stratigraphic, and mineralogic) conditions have made the Takab quadrangle one of the most important metallogenic provinces of Iran, wherein the following mineral deposits/occurrences exist (Ghorbani, 2002):

- Lead–zinc deposits/occurrences, such as Angouran (the largest Zn–Pb mine in the Middle East), Alam Kandi, Poshtkuh, Molla, and Ayghal'esi, with an aggregate of >30 million tons of lead–zinc ores.
- Iron deposits/occurrences, such as Shahrak, Mirjan, Ghaliche Bolagh, Chehar Tagh, Kuhbaba, and Zafarabad, with an estimated aggregate reserve of >50 million tons of iron ores.
- Manganese deposits/occurrences, such as Dabaklou and Amirabad.
- Gold deposits/occurrences, such as Zarshouran, Agh Dare, Zarinabad, and Ghoozlou, and the Arabshah gold indication. Previous investigations show that a minimum of 100 tons of gold occur at Zarshouran and Agh Dare.
- Antimony, arsenic, and mercury deposits/occurrences, such as Moghanlou, Agh Dare, and Ghizghapan antimony deposits, Zarshouran arsenic deposit, Arabshah arsenic indication, Shakh–Shakh mercury indication, and Qare Dash mercury deposit.
- Copper deposits/occurrences, such as Baiche Bagh polymetallic deposit with copper, lead–zinc, cobalt, nickel, and bismuth, and Tataqeshlaqi and Tazekand indications with an estimated ore reserves of 100,000 tons.

4. Geochemical data

A total of 611 stream sediment samples have been collected from within the 1:25,000 scale Takab geological map sheet by the Geological Survey of Iran (GSI) in 2009. In addition, for validation of the reliability of the results of mapping stream sediments geochemical anomalies and, thus, the effectiveness of the geochemical anomaly separation, 40 lithogeochemical samples for chemical analysis were collected from target areas defined in this study (Fig. 2). To evaluate the efficacy of the methods applied, the derived stream sediment geochemical anomalies were compared with the lithogeochemical data for As, Pb, Zn, Cu, Sn, Mo, W, Ni and Sb obtained by XRF (X-ray fluorescence) and Au, Ag, and Hg were analyzed by AAS (flame atomic absorption spectrophotometry). The accuracy of the geochemical data, compared to the Montana soil as standard reference material (SRM) 2710, is 5–10%; whereas the precision, measured by calculating the average difference between duplicate samples (5% of the analyzed samples), is <10%. Analyses were carried out by Geological Survey of Iran (GSI) Laboratories (GSI, 2009). The statistical properties of the element concentrations in the stream sediment samples are given in Table 1, and the skewness coefficients indicate that the raw data are strongly variable probably due to the diversity of lithology and features such as thrusts, faults and mineral occurrences.

5. Results

5.1. Mapping of uni-element anomalies by median + 2MAD method

Concentration values of Au, Pb, Zn and Cu in the 611 stream sediment samples, as favorable metal elements based on the known mineral deposits/occurrences in the Takab area, were used for separating and mapping uni-element geochemical anomalies. The uni-element

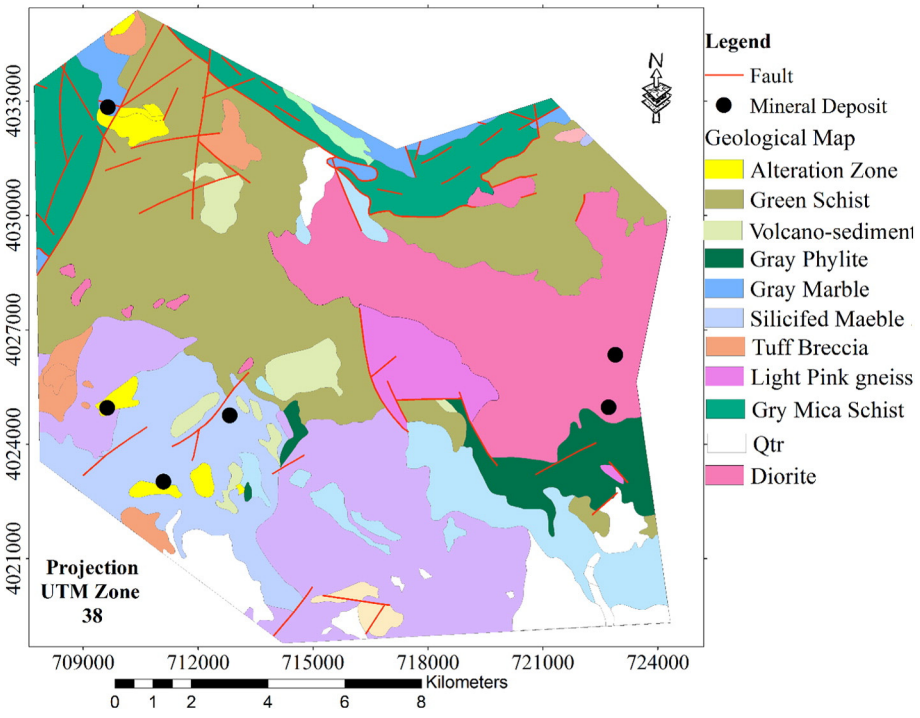

Fig. 1. Simplified geological map of study area – the Takab district.

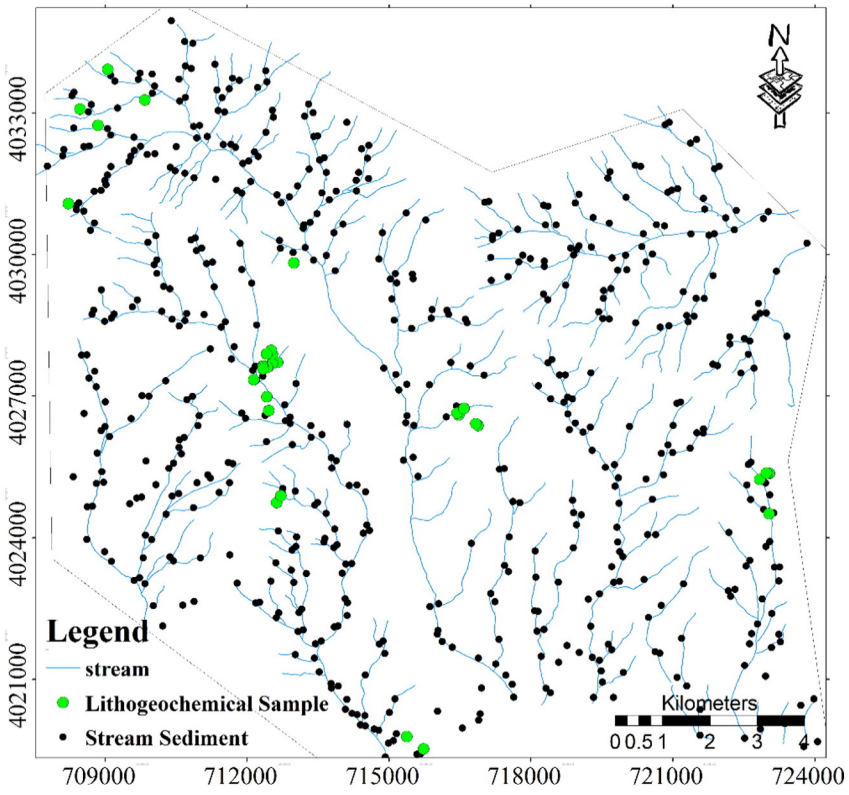

Fig. 2. Locations of stream sediment geochemical samples and lithogeochemical samples.

threshold values obtained using median + 2MAD were used to map the spatial distribution of element concentrations (Fig. 3). These interpolated maps were produced by means of inverse distance weighted (IDW) method.

5.2. Mapping of uni-element anomalies by C-A fractal model

For separation of uni-element geochemical anomalies, the C-A fractal model was applied to stream sediment Au, Pb, Zn and Cu concentration data. Breaks in the straight line segments fitted to the C-A plots of the stream sediment geochemical data (Fig. 4) indicate the presence of two populations in the Au data and three populations in the Pb, Zn, and Cu data. The break point in the C-A plots for the stream sediment Au data define a threshold value, such that the left-hand line segment represents background population (≤11.3 ppb) and the right-hand line segment represents anomalous population of >11.4 ppb (Table 2). Each of the C-A plots for the stream sediment Pb, Zn and Cu data can be modeled with two breaks, such that the left-hand line segments represent background (≤19.95 ppm Pb, ≤95.4 ppm Zn, and ≤35.48 ppm Cu), the middle segments represent moderate anomalies (19.96–1122 ppm Pb, 95.5–416.8 ppm Zn, and 37.15–62.1 Cu), and the right-hand segments represent high anomalies (>1122.1 ppm Pb, >416.9 ppm Zn, and >62.1 ppm Cu) (Table 2). The defined threshold values are then used to reclassify the IDW-interpolated raster maps of the uni-element data (Fig. 5). The multiple thresholds derived by the C-A model represent different geological factors, such as lithological differences, geochemical processes, mineralizations, surficial weathering, which are considered important controls of stream sediment element concentrations (Cheng et al., 1994). Considering the geology of the study area, values of >11.3 ppb Au are correlated with the alteration zone associated with the Chichaklo deposit and the contact zone between silicified marble and gray schist. The Au anomalies also exhibit spatial correlation with faults. The background population of Au (≤11.3 ppb) covers a large portion of the study area underlain by greenschist and diorite (Fig. 5).

The populations of high Pb and Zn anomalies exhibit similar spatial distributions and coincide with the diorite, gray phyllite and partly with gray marble. The populations of moderate Pb and Zn anomalies coincide mainly with greenschist and marbles, and cover large portions of the study area and cannot distinct main anomalies for further

Table 1
Analytical method, detection limit and statistical parameters of favorable elements/metals in the stream sediment geochemical data of the Takab area.

	Number of samples	Detection limit	Minimum	Maximum	Median	MAD
Au (ppb)	611	0.2	1	94	3.23	1.9
Cu (ppm)	611	2.5	8	455	26.6	9.2
Pb (ppm)	611	5	6	7544	44.81	17.6
Zn (ppm)	611	7	26	6850	105.6	42.5
Ag (ppm)	611	0.08	0.05	12.2	0.19	0.08
Sn (ppm)	611	1	1	340	2.5	0.08
Mo (ppm)	611	0.5	0.5	20.1	0.98	0.41
W (ppm)	611	0.5	0.5	10.5	1.07	0.47
Ni (ppm)	611	3	7.5	1150.5	46	15.6
Hg (ppm)	611	0.005	0.01	61	0.06	0.06
As (ppm)	611	2	0.6	2155	32	21
Sb (ppm)	611	0.4	0.14	210	2.65	1.61

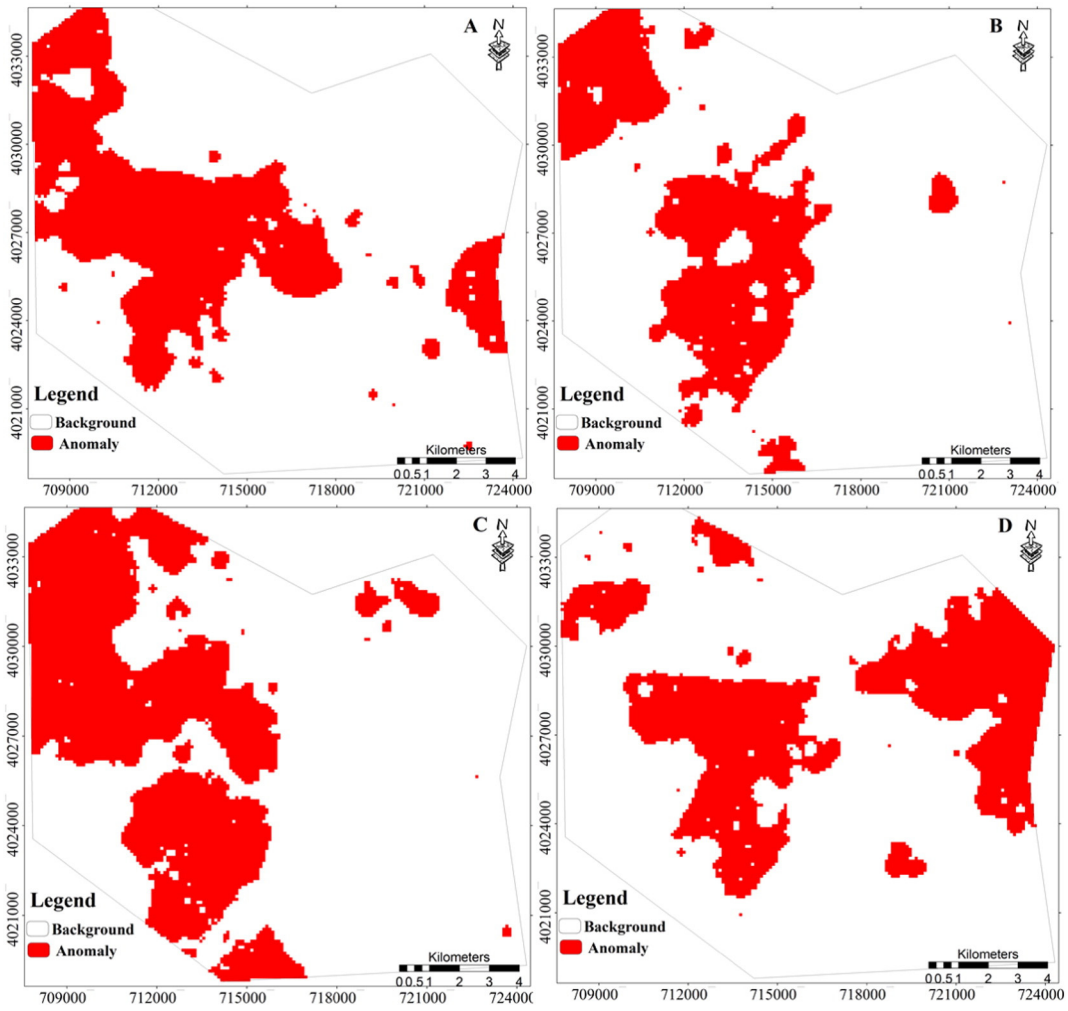

Fig. 3. Uni-element anomaly maps obtained using the median + 2MAD method: (A) Au, (B) Pb, (C) Zn, (D) Cu.

exploration targets. Moreover the spatial distributions of populations of strong anomalies with values ≥1122.1 ppm for Pb and ≥416.9 ppm for Zn indicate that the main mineralization is located near pre-mineralization areas such as Chichaklo and Ayghalesi deposits as well as silicified marbles and volcano-sedimentary rocks. The areas with strong Pb and Zn anomalies are greater than those with Au anomalies, indicating the Pb and Zn are more mobile than the Au in the surface environment of the study area.

The spatial distribution of Cu anomalies based on the thresholds obtained from C-A log-log plots indicate negative correlation with Au, Pb and Zn anomalies but coincides with background for Au, Pb and Zn over limestone and marble rock units. Moderate and strong anomalies of Cu have strong correlation with greenschist and diorite.

Comparison of the spatial distributions of stream sediment anomalous areas for Au, Pb and Zn with those of the lithogeochemical samples indicates that 23% of lithogeochemical samples with lower values of Au defined by C-A method are located in areas of strong anomaly. However, 31% of the lithogeochemical samples with high values of Au are located in background areas. Moderate and strong anomalies are targets for more exploration work. Strong anomalies are mostly associated with silicified marbles and volcano-sedimentary rocks.

Comparison of the spatial distributions of stream sediment Pb anomalies with those of the lithogeochemical samples indicates that 68% of the lithogeochemical samples have Pb values lower than the Pb threshold defined from C-A analysis, and these lithogeochemical samples are located in areas with background and moderate anomalies for Pb in stream sediments. In contrast, 32% of the lithogeochemical samples with Pb values greater than the Pb threshold defined from C-A analysis, and these lithogeochemical samples are located in areas with moderate stream sediment Pb anomalies and just one lithogeochemical sample with high Pb value falling in strong stream sediment Pb anomalies.

Comparison of the spatial distributions of stream sediment Zn anomalies with those of the lithogeochemical samples indicates that 90% of the lithogeochemical samples have Zn values lower than the Zn threshold defined from C-A analysis, and the remaining 10% of lithogeochemical samples with high Zn values coincide with moderate stream sediment Zn anomalies. Comparison of the spatial distributions of stream sediment Au anomalies with those of the lithogeochemical samples indicates that >98% of the lithogeochemical samples have Au values greater than the Au threshold defined from C-A analysis, and these lithogeochemical samples fall in areas with strong stream sediment Au anomalies.

5.3. Mapping of multi-element anomalies by robust PCA and C-A methods

For further evaluation of multi-element geochemical anomalies, by considering the major rock types in the Takab area, data for Cu, Pb, Zn, Au, Ag, Sn, Mo, W, Ni, Mn, Hg, As and Sb were subjected to RPCA. The PC1 and PC2 obtained from RPCA of the ilr-transformed stream sediment geochemical data account for 22% and 16% of total variation, respectively (Table 3; Fig. 4A). The PC1 showed positive loadings for Au, Ag, Pb, Zn, Mn and As (Fig. 6A). PC1 scores were then subjected to C-A fractal modeling and the obtained thresholds were used for

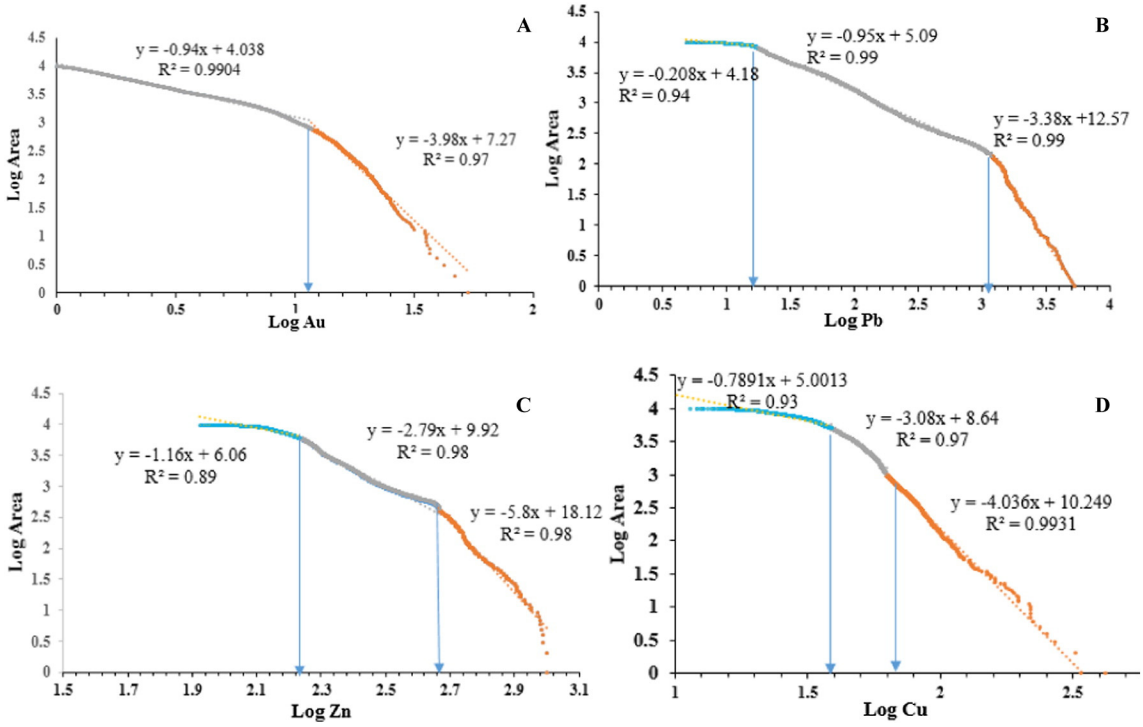

Fig. 4. C-A log-log plots for Au, Pb, Zn and Cu. The vertical axis represents cumulative area $A(\rho)$ occupied by elemental concentrations values greater than ρ, and the horizontal axis is the concentration value ρ.

classification of the PC1 raster map. The reclassified map of PC1 scores indicate that positive loadings are linked to gray marbles and andesitic volcano-sedimentary rocks. Possible represents hydrothermal sediment hosted Pb–Zn mineralization, which is similar to the mineralization in Angouran Pb–Zn giant deposit in the neighboring region. The second assemblage composed of positive loadings of Cu, Mo, Sb, Hg and Ni.

The C-A fractal model was applied to PC1 from robust PCA of stream sediment geochemical data and three line segments, fitted to the C-A log-log plot, were generated (Fig. 6B). Breaks between the straight lines segments and the corresponding values of PC1 loadings have been used as threshold values, to reclassify cell values in the raster geochemical anomaly maps (Fig. 6C). The thresholds on this anomaly map are indicative of three populations, which are interpreted as geologic background, moderate and strong anomalies of multi elements. Strong anomalies of PC1 of robust PCA mainly also coincide with known mineral deposits, silicified marbles and outcrops of hydrothermal alterations. Most low values in the C-A fractal model defined as background and moderate anomalies occur within areas underlain by greenschist and mafic rock outcrops. Comparison of strong anomalies obtained from spatial distribution of PC1 form logratio transformation and C-A fractal model indicate that the later provides a smaller areas for follow-up works and better coincidence with known deposits and altered marbles.

Table 2
Interpretation range of values (ppm) except Au (ppb) of geochemical elements defined by threshold values obtained via concentration-area fractal model.

Element	Concentration value	Interpretation
Au (ppb)	≤11.3	Background
	>11.4	High background
Pb (ppm)	≤19.95	Background
	19.96–1122	Anomaly
	≥1122.1	High anomaly
Zn (ppm)	≤95.4	Background
	95.5–416.8	Anomaly
	≥416.9	High anomaly
Cu (ppm)	≤35.48	Low background
	35.49–62	Background
	≥62.1	Anomaly

5.4. Stepwise regression

As discussed above, we kept predictor variables (X) for which the error (*P-value*) is <0.05 that gives us a 95% level of statistical significance. Table (4) presents the stages of the stepwise regression processes for deriving a multiple regression equation of each of the target elements/metals. The final regression equations for each element/metal are:

$$Au_i = 5.7 + 0.9 \times SiO2_i + 0.6 \times Al2O3_i - 1.2 \times MnO_i \quad (10)$$

$$Pb_i = 89 + 1.54 \times SiO2_i - 0.51 \times Fe2O3_i - 0.14 \times MnO_i \quad (11)$$

$$Zn_i = 291.4 + 2.61 \times SiO2_i + 2.41 \times Al2O3_i + 3.26 \times MnO_i \quad (12)$$

$$Cu_i = 69.1 - 0.8 \times SiO2_i + 8.95 \times Al2O3_i + 11.2 \times Fe2O3_i \quad (13)$$

$$Ag_i = 0.18 - 1.01 \times SiO2_i + 0.9 \times Fe2O3_i + 2.1 \times MnO_i \quad (14)$$

$$Sn_i = 5.1 - 0.9 \times SiO2_i + 3.2 \times Al2O3_i + 0.26 \times Fe2O3_i \quad (15)$$

$$Mo_i = 21.1 - 0.45 \times SiO2_i + 9.21 \times Al2O3_i + 7.58 \times Fe2O3_i \quad (16)$$

$$W_i = 1.9 - 0.09 \times SiO2_i + 0.1 \times MnO_i + 1.4 \times Al2O3_i \quad (17)$$

$$Ni_i = 100 + 0.4 \times SiO2_i - 12.3 \times MnO_i + 13.17 \times Fe2O3_i \quad (18)$$

$$Hg_i = 1.7 - 0.001 \times SiO2_i - 2.6 \times MnO_i + 0.05 \times Fe2O3_i \quad (19)$$

$$As_i = 16.4 - 1.06 \times SiO2_i + 6.2 \times Al2O3_i - 2.2 \times Fe2O3_i \quad (20)$$

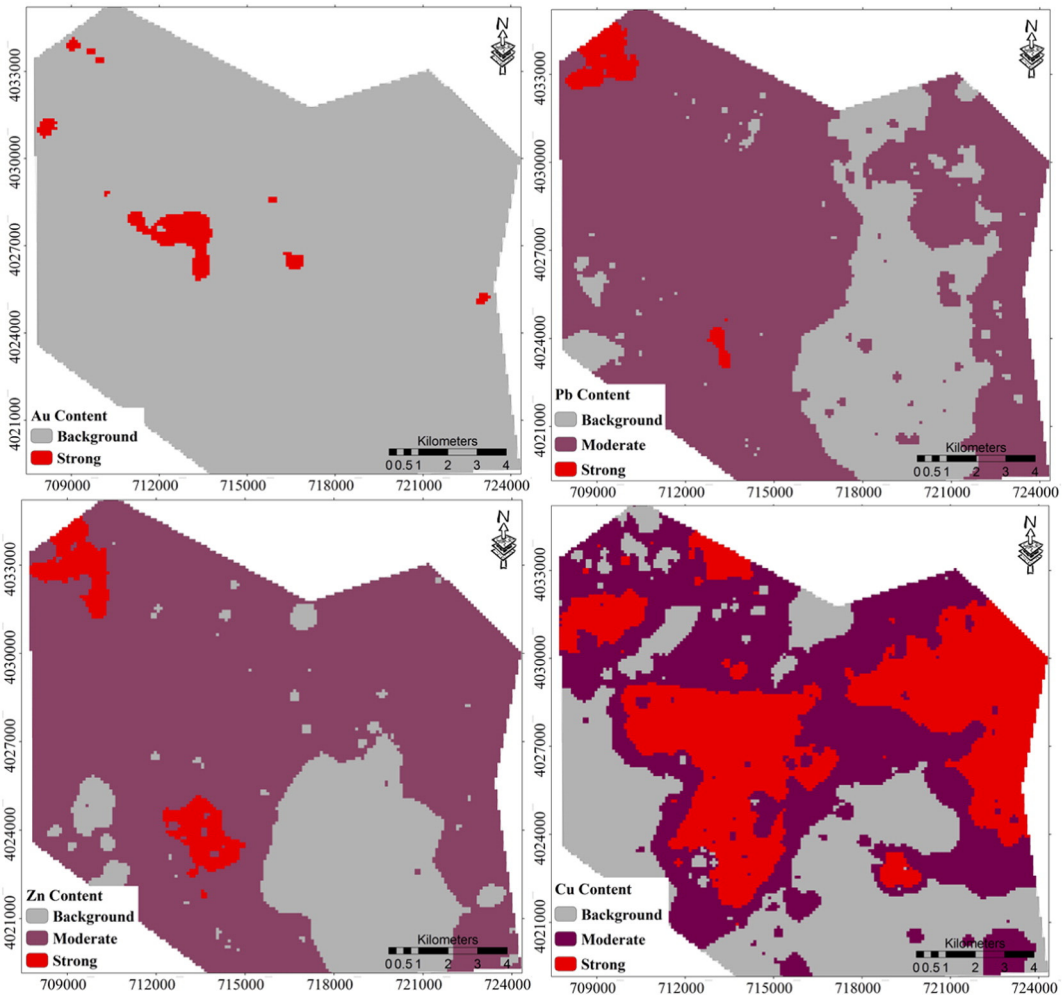

Fig. 5. Maps of spatial distributions of Au, Pb, Zn and Cu based on C-A fractal modeling.

$$Sb_i = -4.9 + 0.22 \times SiO2_i + 18.3 \times Al2O3_i + 0.35 \times Fe2O3_i \quad (21)$$

The above equations were used to calculate predicted values for each of the trace metals at every sample location. The residual values of metals (i.e., measured value minus predicted value) were subjected to PCA and then PCs of interest were subjected to C-A fractal modeling to classify and map multi-element anomalies. The PC1 and PC2 of the residual values account for 45% and 18% of the total variance, respectively (Table 5). The relationship between PC1 and PC2 is shown in the biplot in Fig. 7A. The distribution of samples in biplot form of PC1 and PC2 indicate that the geochemical data do not have closure behavior. Results show positive loadings of Au, As, Pb, and Zn for PC2. The C-A fractal model indicates presence of multiple geochemical anomalies in the PC2 scores of the residual values (Fig. 7B).

Table 3
PCs loadings of the ilr logratio transformed stream sediment geochemical data.

	PC1	PC2	PC3
Au	0.409	0.159	0.236
Cu	−0.218	0.199	0.522
Pb	0.422	0.326	−0.323
Zn	0.229	0.415	−0.404
Ag	0.426	0.227	0.457
Sn	−0.357	0.262	0.13
Mo	0.158	0.349	0.24
W	−0.264	0.151	−0.109
Ni	−0.401	−0.204	0.136
Hg	−0.155	0.317	−0.332
As	−0.417	0.381	−0.144
Sb	0.147	−0.515	0.231
Variance (%)	22	16	11
Cumulative variance	22	38	49

Results of the PCA of residual values portrayed in a biplot (Fig. 7A) and spatial distribution of PC2 (Fig. 7C) indicate that rays of Au, Pb and Zn in the second quadrant are indicator of ground features (silicified lime stone, hydrothermal alteration and volcano sedimentary deposits), which are the primary hosts of Au and Pb–Zn deposits. The third quadrant, which is associated with Cu, Ag, Sn, W and Hg, corresponds to metamorphic and mafic rocks in the study area. The C-A model was employed for further analysis of PC2 (Fig. 7B). Breaks between the straight line segments have been used as threshold values to reclassify the spatial distribution of PC2 (Fig. 7C). Thresholds are indicative of three populations, which are interpreted as background, moderate anomaly and strong anomaly. Similar to the two previous methods approaches, this map also shows strong anomalies are associated with andesitic, trachyandesitic, gray marbles and volcano-sedimentary rock types, also Chichaklo and Ay-Ghale-Si, also hydrothermal zones.

5.5. Validation of stream sediment geochemical anomalies

In order to evaluate the efficiency of the methods used to map stream sediment geochemical anomalies, these anomalies were compared with the lithogeochemical data. Result indicate that there is 100% overlap between Au anomalies delineated using the

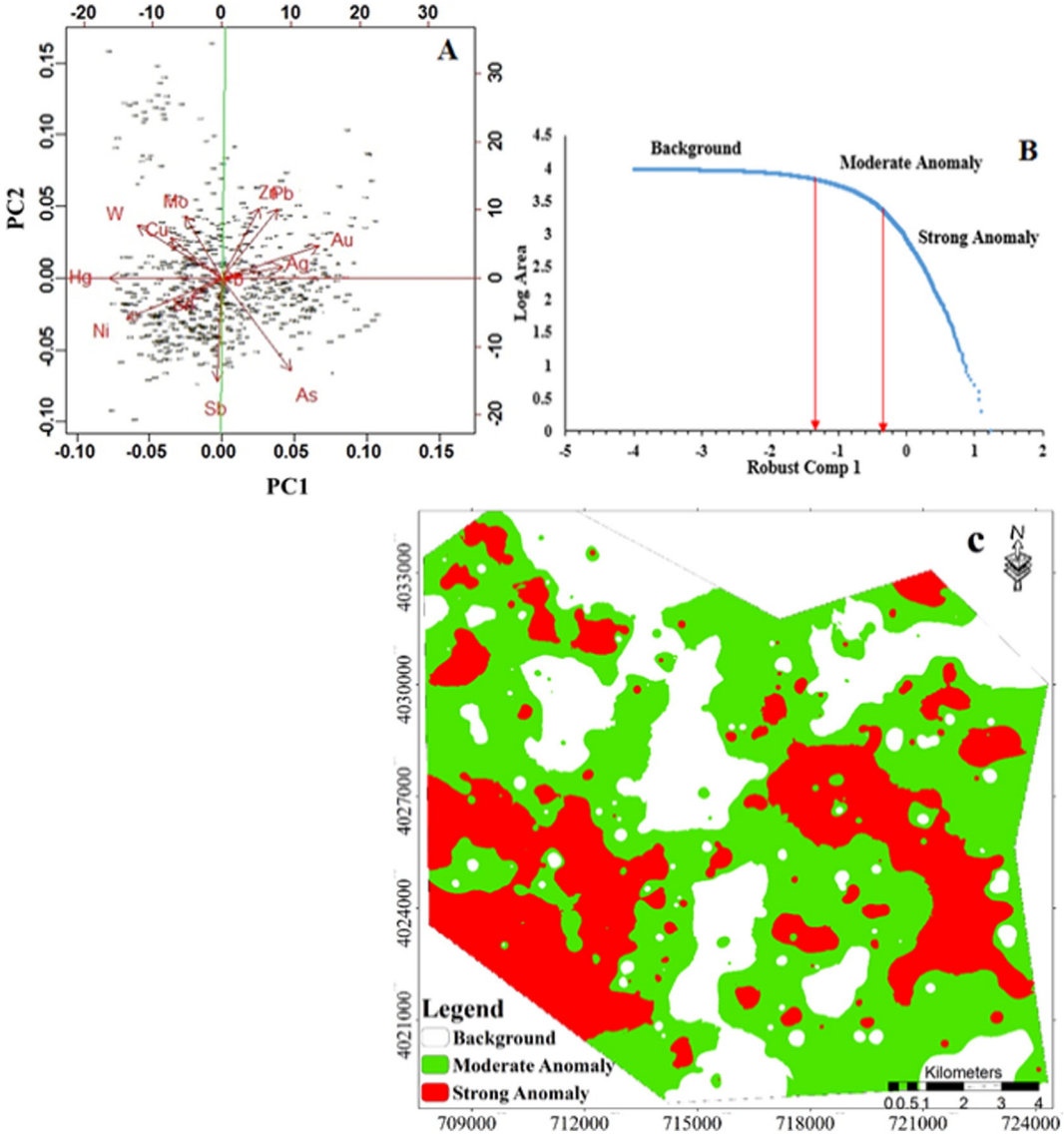

Fig. 6. Results of robust PCA and C-A fractal modeling of multi-element anomalies: (A) biplots of PC1 vs PC2 of multi-elements; (B) C-A log-log plot of PC1 scores; (C) spatial distribution of PC1 scores.

median + 2MAD method and lithogeochemical samples containing >7 ppb Au. However, because of the low Au threshold value obtained using the median + 2MAD method, the anomalous areas cover more than half of study area and so the anomalies are unreliable. Delineated Pb anomalies also indicate 57% overlap for lithogeochemical samples containing >80 ppm Pb, 50% overlap between Zn anomalies and lithogeochemical samples containing >190 ppm Zn, and 77% overlap between Cu anomalies and lithogeochemical samples containing >45 ppm Cu. These results indicate that the presence of stream sediment geochemical anomalies does not always mean the presence of mineral deposits, and as therefore it is necessary to apply certain criteria or the other methods for screening or prioritization of anomalies prior to any follow-up work.

Low values of robust PC1 scores of the stream sediment geochemical data are mainly depicting Cu, Mo, Sb, Hg and Ni, in areas underlain by serpentinite and amphibolite greenschists, whereas high values of robust PC1 scores depict Au, Ag, Pb, Zn, W and As in areas with known deposits or with altered carbonaceous and marble rocks, which are a key geological factor for the formation of sediment-hosted Au and Pb–Zn deposits in the Takab district (Nazarpour et al., 2014). The association of Au, Ag, Pb and Zn thus indicates the most prevalent ground features (i.e., silicified limestones associated with hydrothermal alteration and volcano-sedimentary rocks), which are the primary hosts of Au–As and Pb–Zn mineralization in the study area (Ghorbani, 2002). Therefore, the PC1 of the stream sediment geochemical data represent multiple geological processes such as the lithology, landforms, and mineralization so that further study of the spatial distribution of PC1 scores is needed. The spatial distribution of PC1 scores (Fig. 6C) indicates that high values exist in smaller areas and have good spatial associations with known mineral deposits and outcrops of hydrothermal alterations.

Maps of spatial distribution of uni-element anomalies obtained by median + 2MAD and C-A model of raw geochemical values indicate that the anomalous parts correspond to the andesitic, trachyandesitic lava, gray marbles and volcano-sedimentary rock types. Obtained results indicate that median + 2MAD map for Au separate large area of interest, on the other hand the anomaly map of Au by C-A method coincident with high intense area, where that 23% of lithogeochemical samples with lower values of Au defined by C-A method are located in areas of strong anomaly. Uni-element anomalies of Pb and Zn based on median + 2MAD are approximately similar and cover the areas with andesitic and trachyandesitic lava lithological types. On the other hand, based on C-A method, strong anomalies of Pb and Zn show

Table 4
Stages of the stepwise regression per element/metal.

	Coefficients	Au			Coefficients	Pb		
		Step 1	Step 2	Step 3		Step 1	Step 2	Step 3
		P-value	*P-value*	*P-value*		*P-value*	*P-value*	*P-value*
Intercept	5.70	0.01%	0.01%	0.03%	89.00	0.0%	0.0%	0.1%
SiO_2	0.90	3%	0%	0.04%	1.54	0.0%	4.0%	2.1%
Fe_2O_3	0.87	4.5%	14%		0.51	1.4%	1.1%	0.5%
MgO	0.91	59%			1.39	33.5%		
Al_2O_3	0.60	0.41%	0.01%	0.01%	0.47	23.0%	21.4	
MnO	1.20	0.04%	0.07%	0.00%	0.14	4.1%	3.2%	1.1%
	Coefficients	Zn			Coefficients	Cu		
		Step 1	Step 2	Step 3		Step 1	Step 2	Step 3
		P-value	*P-value*	*P-value*		*P-value*	*P-value*	*P-value*
Intercept	291.40	0.01%	0.08%	0.00%	69.1	0%	0%	0%
SiO_2	2.61	3%	4.1%	0.3%	0.80	0.05%	0.01%	0.00%
Fe_2O_3	22.67	36%			11.2	3.1%	5%	0.05%
MgO	17.50	17%	29%		28.00	29%		
Al_2O_3	2.41	3.4%	1.1%	0.5%	8.95	0.00%	0.00%	0.04%
MnO	3.26	4.1%	3.1%	1.4%	11.20	10%		
	Coefficients	Ag			Coefficients	Sn		
		Step 1	Step 2	Step 3		Step 1	Step 2	Step 3
		P-value	*P-value*	*P-value*		*P-value*	*P-value*	*P-value*
Intercept	0.18	1.1%	2.1%	0.4%	5.10	0%	0%	0%
SiO_2	1.01	1.10%	2.2%	1.4%	0.90	0.05%	0%	0%
Fe_2O_3	0.90	4.5%	0.0%	0.0%	0.26	3%	0.14%	0%
MgO	13.40	29%			4.50	29%		
Al_2O_3	12.24	0.00%	0.00%	0.04%	3.20	0.00%	0.00%	0.04%
MnO	2.10	16%			7.40	4%	15%	
	Coefficients	W			Coefficients	Mo		
		Step 1	Step 2	Step 3		Step 1	Step 2	Step 3
		P-value	*P-value*	*P-value*		*P-value*	*P-value*	*P-value*
Intercept	1.90	0%	0%	0%	21.10	0%	0%	0%
SiO_2	0.09	0.05%	0.01%	0.08%	0.45	3.1%	2.1%	0%
Fe_2O_3	0.70	4.1%	17%		7.58	4.5%	8.4%	
MgO	0.10	29%			1.40	29%		
Al_2O_3	1.40	0.00%	0.00%	0.04%	9.21	0.00%	0.10%	0.04%
MnO	0.10	3.2%	1.5%	0.05%	4.61	10%	0%	0%
	Coefficients	Ni			Coefficients	Hg		
		Step 1	Step 2	Step 3		Step 1	Step 2	Step 3
		P-value	*P-value*	*P-value*		*P-value*	*P-value*	*P-value*
Intercept	100.0	0%	0%	0%	1.70	0%	0%	0%
SiO_2	0.40	2.4%	0%	0%	0.001	0.05%	0%	0%
Fe_2O_3	13.17	15%			0.05	2.4%	14%	
MgO	28.00	29%			12.40	29%		
Al_2O_3	8.95	0.00%	0.0%	0.04%	6.70	2.40%	0.15%	0.10%
MnO	12.30	10%	0%	0%	2.60	0.0%	1.1%	2.2%
	Coefficients	As			Coefficients	Sb		
		Step 1	Step 2	Step 3		Step 1	Step 2	Step 3
		P-value	*P-value*	*P-value*		*P-value*	*P-value*	*P-value*
Intercept	16.40	0%	0%	0%	−4.90	0%	0%	0%
SiO_2	1.06	0.05%	3%	2.4%	0.22	4%	0.04%	0.00%
Fe_2O_3	2.20	0%	0%	3.1%	0.35	3.8%	2%	0%
MgO	28.00	29%			28.00	29%		
Al_2O_3	6.20	0.00%	0.00%	0.04%	18.30	0.00%	0.00%	0.04%
MnO	11.20	4.1%	14.6%		6.74	9.8%		

small areas of interest. The strong anomaly of Pb shows that 32% of lithogeochemical samples have greater values than defined threshold that located in moderate zone and just one sample with high value of Pb falls in strong anomalies, while correlation between the Zn anomalies by C-A method and lithogeochemical samples shows that 90% of lithogeochemical samples have lower values than defined threshold and remaining 10% of samples with high values correlate with moderate anomalous area.

Results of the stepwise regression for PC2 that is linked with Au, Pb and Zn reveal that the separated anomalies have good spatial association with the andesitic rocks, recrystallized limestone, white-thickly bedded dolomite, altered dark and light gray marble occurrences,

Table 5
Results of PCA of geochemical residuals of stream sediment geochemical data derived by stepwise multiple regression.

	PC1	PC2	PC3
Au	−0.312	0.405	−0.234
Cu	−0.312	0.353	0.11
Pb	−0.424	−0.272	0.278
Zn	−0.46	−0.166	0.174
Ag	−0.465	−0.204	0.214
Ni	0.251	0.441	−0.488
Sb	−0.367	0.129	−0.158
Mo	−0.543	0.197	0.192
W	−0.212	0.32	−0.532
Ni	−0.522	0.248	0.233
Sn	−0.301	−0.476	−0.426
Hg	0.186	0.8	−0.492
As	−0.56	−0.155	−0.112
Variance (%)	45	18	10
Cumulative variance	45	63	73

which are the main host rocks of Pb and Zn occurrences such as Chichaklo and Ay-Ghale-Si and the Angouran major giant Pb–Zn deposit in the Takab district. Validation of delineated multi-element anomalies derived by stepwise regression against the lithogeochemical samples indicate that approximately 100% of lithogeochemical samples fall with high Pb, Zn, and Au values into the delineated strong anomaly domains derived from stepwise regression. Therefore, delineation of robust anomalies of Au and Pb, Zn by stepwise regression, indicate new target areas for further exploration work. The above results suggest that the median + 2MAD and C-A methods are significantly impacted by lithology, although the influence of lithology can be eliminated to a considerable extent by using the presented method in this paper.

Finally, results indicate that the median + 2MAD and C-A methods are useful within a region with simple geochemical background, but they have some limitations within a region linked with complex geological setting. This statement also has been proved by Zuo et al. (2013b) in comparison of C-A and S-A models. When the study area is regarded a whole mineral district regardless of different geological background and different geochemical field in a complex region, the C-A model could not well identify anomalies. However, comparison of results of multi-element geochemical anomalies by robust PCA and stepwise regression indicate that multi-element anomalies of stream sediment geochemical residuals do not only have good correspondence with 100% of lithogeochemical samples with high metal values but also introduce new target areas for further exploration work.

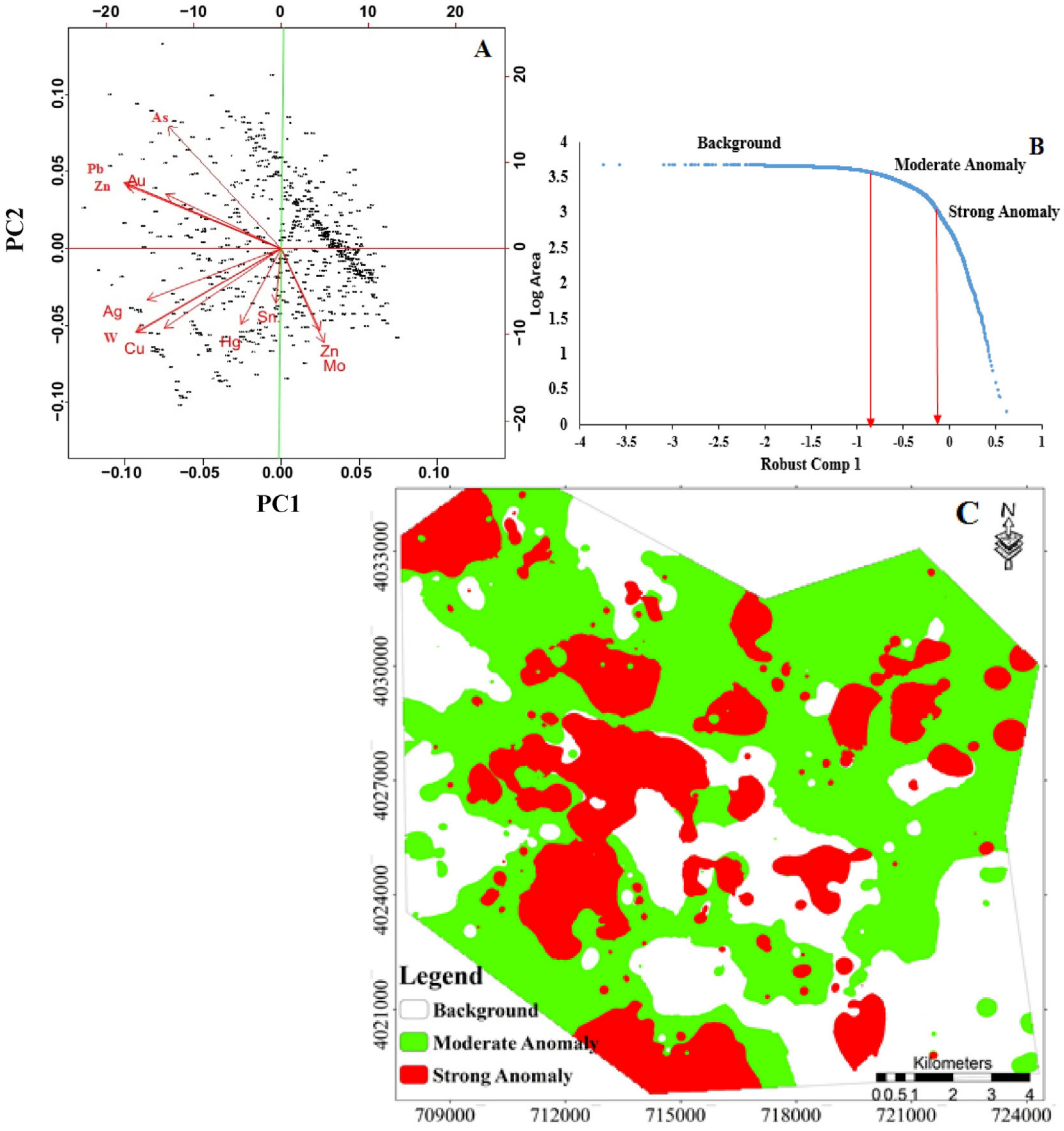

Fig. 7. Results of stepwise regression, robust PCA and C-A fractal modeling of multi-element anomalies: (A) biplot of PC1 vs PC2 of estimated values from stepwise regression; (B) C-A log-log plot of PC1 scores of estimated values from stepwise regression; (C) spatial distribution of PC1 scores of estimated values from stepwise regression.

6. Conclusions

In this paper, stepwise multiple regression was used to delineate anomalies using geochemical residuals of trace metals in an area with variable lithological types depicting a complex geological setting. For comparative analysis and reliability control of obtained anomalous areas derived by using geochemical residuals, we used (i) robust median + 2MAD as a technique of exploratory data analysis, (ii) concentration-area (C-A) fractal modeling and (iii) robust PCA. Comparison of delineated geochemical anomalies based of median + 2MAD and C-A modeling with those obtaining based on robust PCA and stepwise method indicates that the first two methods are more influenced by lithology and are inadequate for identifying geochemical anomalies in areas with variable lithology. The application of robust PCA on geochemical residuals derived by stepwise multiple regression using major oxides as predictors of trace metals to eliminate lithology effects is powerful tool to identify geochemical anomalies in areas with variable lithological types and complex geological setting. This approach also indicate that, in the study area, mapped multi-element anomalies are not only associated with known deposits such as Chichaklo and Ay-Ghale-Si deposits but also are linked with structural features reflecting the existence of new target areas of interest.

References

Afzal, P., Khakzad, A., Moarefvand, P., Omran, N.R., Esfandiari, B., Alghalandis, Y.F., 2010. Geochemical anomaly separation by multifractal modeling in Kahang (Gor Gor) porphyry system, Central Iran. J. Geochem. Explor. 104, 34–46.

Afzal, P., Fadakar Alghalandis, Y., Khakzad, A., Moarefvand, P., Rashidnejad Omran, N., 2011. Delineation of mineralization zones in porphyry Cu deposits by fractal concentration–volume modeling. J. Geochem. Explor. 108, 220–232.

Agard, P., Omrani, J., Jolivet, L., Mouthereau, F., 2005. Convergence history across Zagros (Iran): constraints from collisional and earlier deformation. Int. J. Earth Sci. 94, 401–419.

Agterberg, F., 1995. Multifractal modeling of the sizes and grades of giant and supergiant deposits. Int. Geol. Rev. 37, 1–8.

Agterberg, F., Cheng, Q., Wright, D., 1993. Fractal Modeling of Mineral Deposits, 24th APCOM Symposium Proceeding. Montreal, Canada, pp. 43–53.

Aitchison, J., 1986. The Statistical Analysis of Compositional Data. Springer.

Ali, K., Cheng, Q., Chen, Z., 2007. Multifractal power spectrum and singularity analysis for modelling stream sediment geochemical distribution patterns to identify anomalies related to gold mineralization in Yunnan Province, South China. Geochem. Explor. Environ. Anal. 7, 293–301.

Asadi, H.H., Kianpouryan, S., Lu, Y.-J., McCuaig, T.C., 2014. Exploratory data analysis and C–A fractal model applied in mapping multi-element soil anomalies for drilling: a case study from the Sari Gunay epithermal gold deposit, NW Iran. J. Geochem. Explor. 145, 233–241.

Bonham-Carter, G., Goodfellow, W.D., 1984. Autocorrelation structure of stream sediment geochemical data: interpretation of zinc and lead anomalies, Nahanni river area, Yukon-Northwest Territories, Canada. In: Verly, G., et al. (Eds.), Geostatistics for Natural Resources Characterization, Part 2. D. Reidel, Dordrecht, pp. 817–829.

Bonham-Carter, G.F., Goodfellow, W.D., 1986. Background corrections to stream geochemical data using digitized drainage and geological maps: application to Selwyn Basin, Yukon and Northwest Territories. J. Geochem. Explor. 25 (1–2), 139–155.

Carranza, E.J.M., 2008. Geochemical Anomaly and Mineral Prospectivity Mapping in GIS. Elsevier.

Carranza, E.J.M., 2010a. Catchment basin modelling of stream sediment anomalies revisited: incorporation of EDA and fractal analysis. Geochem. Explor. Environ. Anal. 10, 365–381.

Carranza, E.J.M., 2010b. Mapping of anomalies in continuous and discrete fields of stream sediment geochemical landscapes. Geochem. Explor. Environ. Anal. 10, 171–187.

Carranza, E.J.M., 2011. Analysis and mapping of geochemical anomalies using logratio-transformed stream sediment data with censored values. J. Geochem. Explor. 110, 167–185.

Carranza, E.J.M., Hale, M., 1997. A catchment basin approach to the analysis of geochemical-geological data from Albay province, Philippines. J. Geochem. Explor. 60 (2), 157–171.

Cheng, Q., 2004. A new model for quantifying anisotropic scale invariance and for decomposition of mixing patterns. Math. Geol. 36, 345–360.

Cheng, Q., 2007. Mapping singularities with stream sediment geochemical data for prediction of undiscovered mineral deposits in Gejiu, Yunnan Province, China. Ore Geol. Rev. 32, 314–324.

Cheng, Q., Agterberg, F., Ballantyne, S., 1994. The separation of geochemical anomalies from background by fractal methods. J. Geochem. Explor. 51, 109–130.

Cheng, Q., Xu, Y., Grunsky, E., 2000. Integrated spatial and spectrum method for geochemical anomaly separation. Nat. Resour. Res. 9, 43–52.

Cohen, D.R., Rutherford, N.F., Morisseau, E., Christoforou, I., Zissimos, A.M., 2012. Anthropogenic versus lithological influences on soil geochemical patterns in Cyprus. Geochem. Explor. Environ. Anal. 12, 349–360.

De Vivo, B., Boni, M., Costabile, S., 1998. Formational anomalies versus mining pollution: geochemical risk maps of Sardinia, Italy. J. Geochem. Explor. 64, 321–337.

Deng, J., Wang, Q., Yang, L., Wang, Y., Gong, Q., Liu, H., 2010. Delineation and explanation of geochemical anomalies using fractal models in the Heqing area, Yunnan Province, China. J. Geochem. Explor. 105, 95–105.

Egozcue, J.J., Pawlowsky-Glahn, V., Mateu-Figueras, G., Barceló-Vidal, C., 2003. Isometric logratio transformations for compositional data analysis. Math. Geol. 35, 279–300.

Filzmoser, P., Hron, K., Reimann, C., 2009. Univariate statistical analysis of environmental (compositional) data: problems and possibilities. Sci. Total Environ. 407, 6100–6108.

Filzmoser, P., Hron, K., Reimann, C., 2010. The bivariate statistical analysis of environmental (compositional) data. Sci. Total Environ. 408, 4230–4238.

Ghasemi, A., Talbot, C., 2006. A new tectonic scenario for the Sanandaj–Sirjan Zone (Iran). J. Asian Earth Sci. 26, 683–693.

Ghorbani, M., 2002. An Introduction to Economic Geology of Iran. National Geosciences Database of Iran (NGDIR).

Geological Survey of Iran, 2009. Stream sediment geochemical exploration in Takab area (1:25,000 scale). internal report Tehran.

Govett, G., Goodfellow, W., Chapman, R., Chork, C., 1975. Exploration geochemistry—distribution of elements and recognition of anomalies. J. Int. Assoc. Math. Geol. 7, 415–446.

Hao, L., Zhao, X., Zhao, Y., Lu, J., Sun, L., 2014. Determination of the geochemical background and anomalies in areas with variable lithologies. J. Geochem. Explor. 139, 177–182.

Hawkes, H.E., Webb, J.S., 1962. Geochemistry in Mineral Exploration.

Jolliffe, I., 2002. Principal Component Analysis. Wiley Online Library.

Kaiser, Henry F., 1960. The application of electronic computers to factor analysis. Educational and psychological measurement.

Karimzadeh Somarin, A., 2005. Petrology and geochemistry of Early Tertiary volcanism of the Mendejin area, Iran, and implications for magma genesis and tectonomagmatic setting. Geodin. Acta 18, 343–362.

Kürzl, H., 1988. Exploratory data analysis: recent advances for the interpretation of geochemical data. J. Geochem. Explor. 30, 309–322.

Li, C., Ma, T., Shi, J., 2003. Application of a fractal method relating concentrations and distances for separation of geochemical anomalies from background. J. Geochem. Explor. 77, 167–175.

Locantore, N., Marron, J., Simpson, D., Tripoli, N., Zhang, J., Cohen, K., Boente, G., Fraiman, R., Brumback, B., Croux, C., 1999. Robust principal component analysis for functional data. TEST 8, 1–73.

Mandelbrot, B.B., 1983. The Fractal Geometry of Nature. Macmillan.

Miesch, A., 1981. Estimation of the geochemical threshold and its statistical significance. J. Geochem. Explor. 16, 49–76.

Mohajjel, M., Fergusson, C.L., 2000. Dextral transpression in Late Cretaceous continental collision, Sanandaj–Sirjan zone, western Iran. J. Struct. Geol. 22, 1125–1139.

Moon, C.J., 1999. Towards a quantitative model of downstream dilution of point source geochemical anomalies. J. Geochem. Explor. 65, 111–132.

Nabavi, M., 1976. An introduction to the geology of Iran. Geol. Surv. Iran 109.

Nazarpour, A., Omran, N.R., Paydar, G.R., 2015a. Application of multifractal models to identify geochemical anomalies in Zarshuran Au deposit, NW Iran. Arab. J. Geosci. 1–13.

Nazarpour, A., Omran, N.R., Paydar, G.R., Sadeghi, B., Matroud, F., Nejad, A.M., 2015b. Application of classical statistics, logratio transformation and multifractal approaches to delineate geochemical anomalies in the Zarshuran gold district, NW Iran. Chem. Erde-Geochem.

Nazarpour, A., Sadeghi, B., Sadeghi, M., 2015c. Application of fractal models to characterization and evaluation of vertical distribution of geochemical data in Zarshuran gold deposit, NW Iran. J. Geochem. Explor. 148, 60–70.

Ohta, A., Imai, N., Terashima, S., Tachibana, 2005. Influence of surface geology and mineral deposits on the spatial distributions of elemental concentrations in the stream sediments of Hokkaido, Japan. J. Geochem. Explor. 86, 86–103.

Pazand, K., Hezarkhani, A., Ataei, M., Ghanbari, Y., 2011. Application of multifractal modeling technique in systematic geochemical stream sediment survey to identify copper anomalies: a case study from Ahar, Azarbaijan, Northwest Iran. Chem. Erde-Geochem. 71, 397–402.

Rantitsch, G., 2000. Application of fuzzy clusters to quantify lithological background concentrations in stream-sediment geochemistry. J. Geochem. Explor. 71, 73–82.

Reimann, C., Garrett, R.G., 2005. Geochemical background—concept and reality. Sci. Total Environ. 350, 12–27.

Rezaei, S., Lotfi, M., Afzal, P., Jafari, M.R., Shamseddin Meigoony, M., 2015. Delineation of Cu prospects utilizing multifractal modeling and stepwise factor analysis in Noubaran 1:100,000 sheet, Center of Iran. Arab. J. Geosci. 8 (9), 7343–7357.

Shacham, M., 1999. Regression diagnostic using an orthogonalized variables based stepwise regression procedure. Comput. Chem. Eng. 23, S327–S330.

Shacham, M., Brauner, N., 2003. The SROV program for data analysis and regression model identification. Comput. Chem. Eng. 27 (5), 701–714.

Shamseddin Meigoony, M., Afzal, P., Gholinejad, M., Yasrebi, A.B., Sadeghi, B., 2014. Delineation of geochemical anomalies using factor analysis and multifractal modeling based on stream sediments data in Sarajeh 1:100,000 sheet, Central Iran. Arab. J. Geosci. 7, 5333–5343.

Sim, B., Agterberg, F.P., Beaudry, C., 1999. Determining the cutoff between background and relative base metal smelter contamination levels using multifractal methods. Comput. Geosci. 25, 1023–1041.

Sinclair, A.J., 1976. Applications of Probability Graphs in Mineral Exploration. Association of Exploration Geochemists.
Stanley, C.R., Sinclair, A.J., 1989. Comparison of probability plots and the gap statistic in the selection of thresholds for exploration geochemistry data. J. Geochem. Explor. 32, 355–357.
Tukey J.W., 1977. Exploratory Data Analysis. Addison-Wesley Massachusetts.
Turcotte, D.L., 1986. A fractal approach to the relationship between ore grade and tonnage. Econ. Geol. 81, 1528–1532.
Turcotte, D.L., 2002. Fractals in petrology. Lithos 65, 261–271.
Wang, H., Zuo, R., 2015. A comparative study of trend surface analysis and spectrum-area multifractal model to identify geochemical anomalies. J. Geochem. Explor.
Wang, Q., Deng, J., Liu, H., Yang, L., Wan, L., Zhang, R., 2010. Fractal models for ore reserve estimation. Ore Geol. Rev. 37, 2–14.
Wei, B., Yang, L., 2010. A review of heavy metal contaminations in urban soils, urban road dusts and agricultural soils from China. Microchem. J. 94, 99–107.
Xu, Y., Cheng, Q., 2001. A fractal filtering technique for processing regional geochemical maps for mineral exploration. Geochem. Explor. Environ. Anal. 1, 147–156.
Zheng, Y., Sun, X., Gao, S., Wang, C., Zhao, Z., Wu, S., Li, J., Wu, X., 2014. Analysis of stream sediment data for exploring the Zhunuo porphyry Cu deposit, southern Tibet. J. Geochem. Explor. 143, 19–30.
Zuo, R., Xia, Q., Zhang, D., 2013b. A comparison study of the C–A and S–A models with singularity analysis to identify geochemical anomalies in covered areas. Appl. Geochem. 33, 165–172.